Coupling of demixing and magnetic ordering phase transitions probed by turbidimetric measurements in a binary mixture doped with magnetic nanoparticles

2010 J. Phys.: Condens. Matter 22 195101

(http://iopscience.iop.org/0953-8984/22/19/195101)

IOP Publishing Journal of Physics: Condensed Matter

J. Phys.: Condens. Matter **22** (2010) 195101 (10pp) doi:10.1088/0953-8984/22/19/195101

Coupling of demixing and magnetic ordering phase transitions probed by turbidimetric measurements in a binary mixture doped with magnetic nanoparticles

Lorenzo Hernández-Díaz, Juan Carlos Hernández-Reta, Armando Encinas and Yuri Nahmad-Molinari[1]

Instituto de Física, Universidad Autónoma de San Luis Potosí, Álvaro Obregón 64, 78000 San Luis Potosí, Mexico

E-mail: yuri@ifisica.uaslp.mx

Received 4 November 2009, in final form 11 March 2010
Published 16 April 2010
Online at stacks.iop.org/JPhysCM/22/195101

Abstract

We present a novel study on the effect of a magnetic field applied on a binary mixture doped with magnetic nanoparticles close to its demixing transition. Turbidity measurements in the Faraday configuration show that the effect of applying an external field produces changes in the critical opalescence of the mixture that allow us to track an aggregation produced by critical Casimir forces and a reversible aggregation due to the formation of chain-like flocks in response to the external magnetic field. The observation of a crossover of the aggregation curves through optical signals is interpreted as the evolution from low to high power dispersion nuclei due to an increase in the radius of the condensation seed brought about by Casimir or magnetic interactions. Finally, evidence of an enhanced magnetocaloric effect due to the coupling between mixing and ordering phase transitions is presented which opens up a nonsolid state approach of designing refrigerating cycles and devices.

(Some figures in this article are in colour only in the electronic version)

1. Introduction

Arising from electrodynamic quantum fluctuations of vacuum along with the boundary conditions imposed by two dielectric or conducting plates, there is an attraction between the considered surfaces first predicted by Casimir and Polder [1]. These forces can be measured in analogous systems in which electromagnetic fluctuations of the zero field in vacuum are replaced by fluctuations in the composition within a critical mixture close to its demixing transition, the so-called critical Casimir forces, first predicted by Fisher and de Gennes and then calculated by Schlesener *et al* [2]. The search for measuring and the control of these critical Casimir forces has guided the community to study colloidal particles suspended in critical mixtures [3], and gave striking results recently when, for the first time, these forces were directly measured by Hertlein *et al* [4] by means of trapping with optical tweezers close to a plane surface, a colloidal particle suspended on a binary mixture close to its critical point.

Furthermore, demixing of binary mixtures of liquids and alloys is a topic of great interest both in applied as well as in fundamental physical chemistry and metallurgy. Controlling the critical demixing temperature by means of an external magnetic field is an attractive goal for many industrial processes. However, in spite of many attempts, using, for example, high gradients and intense electric or magnetic fields, only modest changes in the critical temperature have been achieved [5].

[1] Author to whom any correspondence should be addressed.

On the other hand, magnetic separation is a widely used method for valuable mineral and metal recovery, and drug delivery magnetic nanodevices have been proposed. From our point of view, the use of these magnetic nanoparticles with tailored surface properties and interaction potentials for separation purposes represents a task of major impact in industrial activity, spanning from the chemical and pharmaceutical up to the metallurgical and mining processes of nonmagnetic values. In this scenario, the possibility of controlling the separation temperature of a partially miscible mixture by an imposed magnetic field, and in turn the colloidal interactions within a suspension, opens up a completely new and innovative field to design separation processes.

Magnetically induced ordering of particles in response to an imposed external magnetic field is a field of broad interest in studies that span from magnetorheological fluids to magneto-optical devices and, for example, the development of ferrofluids was a mayor challenge during the past decade [6, 7]. This induced ordering is used in dampers full of a magnetorheological fluid in which the viscosity can be changed by several orders of magnitude as an external magnetic field is imposed. This control of the rheological properties is used for intelligent damping devices that respond proportionally to the applied shear rate and has been implemented for giving aerodynamic stability to bridges or buildings and in the automotive industry for autoadaptable suspensions to rough or smooth roads.

The influence of an external magnetic field on materials could affect other intrinsic properties such as the permittivity tensor and, as a consequence, the way in which electromagnetic radiation interacts with the material. In this case, ellipsometric or turbidimetric changes can be detected [8] depending on the scale on which this tensor is described, being a molecular or an effective-like medium or mesoscopic description of the material media.

These external magnetic fields also alter the orientational distribution of magnetic dipolar moments within a material, which requires energy to proceed inducing heat transfer, a phenomenon called the magnetocaloric effect. Since 1927, when the fundamental principle of adiabatic demagnetization was suggested by Debye and Giauque [9], there has been an enormous effort to obtain materials with a magnetocaloric effect strong enough to allow its usage within a refrigeration cycle at room temperature [10]. This process by which the removal of a magnetic field from certain materials serves to lower their temperature implies that some heat from the sample is spent in disordering the dipoles ordered by the application of the field—energy (and entropy) transfers from thermal entropy to magnetic entropy (disorder of the magnetic dipoles)—and has led to important achievements such as reaching millikelvin temperatures in cryogenic experiments [11].

In this paper we present optical measurements that give information on the coupling of the demixing and magnetic ordering phase transitions in a binary mixture of two partially miscible liquids doped with superparamagnetic nanoscopic particles. Our fundamental hypothesis was that magneto-optical and, very likely, magnetocaloric effects can be enhanced by coupling the ordering of magnetic particles in response to a magnetic field close to the demixing transition of a binary mixture of two partially miscible liquids.

2. Materials and methods

In order to measure changes in transmittance of the samples close to their demixing transition in response to an external magnetic field, a thermally isolated cell is connected to a water flux coming from a constant temperature bath. This cell in turn works as a thermal bath with the sample positioned in its center and allowing the light to pass through due to a couple of optical windows. The cell with the sample was placed in the central region of a pair of Helmholtz coils of 30 cm in diameter, which can produce uniform magnetic fields up to 100 Oe at the position where the sample is located. A 5 mW He–Ne laser (JDS Uniphase) at 633 nm was aligned to the Helmholtz coils' axis in a Faraday-like configuration. The laser beam is divided into two equally intense beams by means of a 50% beamsplitter cube before crossing through the thermal bath cell and the sample itself. One beam is used as a reference in order to eliminate stray light signals or fluctuations of the laser, while the second is used to probe the optical properties of the binary mixture. Each beam impinges on a photodiode and their output signal is amplified before reading with an Agilent bench top multimeter, which is connected to an HPIB-USB board for data acquisition in a PC. The output signal acquired by the computer is the quotient between the probing and the reference beam intensities. Also, a thermocouple located within the cell and connected to a second digital multimeter registers the actual temperature of the sample using the same HPIB protocol. With this set-up, we were able to directly measure curves of transmittance or directly measure the transmitted intensity (without a reference signal) as a function of temperature with cooling rates or ramps of about 10 mK s^{-1} and for different values of the applied magnetic field.

Five milliliter samples of different compositions of the doped binary mixture made of cyclohexane–methanol ranging from 0.2 up to 0.75 in the volume fraction of methanol were prepared in clean borosilicate test tubes. The components used were 99.9% pure reagent grade cyclohexane (CH) and methanol provided by Sigma and used as received. The cyclohexane has been doped with magnetic nanoparticles by adding 10 μl of commercial grade ferrofluid to 50 ml of cyclohexane. The magnetic dopant was Ferrosound ferrofluid EFH1 from Ferrotec, which is a stable suspension of magnetite nanoparticles, with an average diameter of 10 nm as reported by the company, suspended in hydrocarbon synthetic oil. It is worth noting that, since the suspension is stable for high intensity field applications (magnetic seals and bearings, loudspeakers, etc), the colloidal steric Rosensweig stabilizing barrier should be larger than the magnetic interaction at saturation (2 kOe), typically of the order of $300k_BT$ (where this ratio is given numerically by the total number of molecules of the dispersant agent adsorbed onto the whole surface of a spherical particle) [7]. Since we are working at much lower magnetic fields (80 Oe) and the dipolar interaction scales with the squared magnetic moment, we are working with

interactions a thousand times weaker than those for which the commercial ferrofluid was designed to be stable.

This means that, for these very low intensity fields used during our experiments, we were far from overcoming the irreversible aggregation barrier, but the normal dispersion power of magnetite particles is already enough to produce magneto-optic effects [12]. On the other hand, the size of the ferrofluid particles would be in the limit of aggregation if no steric barrier were present. That is, they are in the limit for which the quotient

$$\frac{\text{thermal energy}}{\text{dipole–dipole energy at contact}} = \frac{12k_{\mathrm{B}}T}{\mu_0 M^2 V} \tag{1}$$

where k_{B} is the Boltzmann constant, T the absolute temperature, μ_0 is the permeability of free space, M the intensity of magnetization and V the volume of a particle, is close to one for magnetite particles, since equation (1) requires a diameter:

$$d \leqslant \left(\frac{72k_{\mathrm{B}}T}{\pi\mu_0 M^2}\right)^{1/3} = 7.8\ \text{nm} \tag{2}$$

in order to prevent them from thermal aggregation.

Preparation of different compositions was done by volume in a dry environment. It should be noticed that the doping magnetite particles either in cyclohexane or in the cyclohexane–methanol mixture remain stable even for several months at room temperature (below the mixed states) as long as the process of mixing/demixing does not takes place. This means that the surfactant agent remains covering the magnetic particles after they have been resuspended in the cyclohexane phase, keeping them stable due to steric repulsion.

The particle size and zeta potential of a very diluted sample of these nanoparticles resuspended in cyclohexane was measured by means of a Malvern Equipment, model ZEN-3600, giving an average of 31 nm in hydrodynamic diameter with a very narrow distribution, and a zeta potential of −0.0886 mV which can be interpreted as a negligible surface charge density or electrostatic stabilization mechanism.

The growth of magnetic suspended particles by irreversible aggregation produces aging of the samples that become unusable for further tests. In our experiments, care was taken in keeping and ensuring identical conditions during sample preparation in order to avoid any shifting in the phase diagram produced by humidity traces and clearly distinguishes the magnetic field effects from those produced by humidity traces. Our principal aim was to measure a change of the optical properties of the mixture close to phase separation in response to an applied external magnetic field. This was done for six different compositions using fresh samples in each run due to possible aging effects (as was observed). This means that one has to perform a first cooling cycle with a fresh sample under the applied magnetic field and then a second cooling cycle using a new, identical fresh sample without the magnetic field. The reason for this protocol is evident from the observation of magnetic nanoparticles precipitating as heating and cooling cycles proceeded, changing in turn the effective composition of the binary (truly ternary) system. In other words, the magnetic particles suspended in the binary mixture

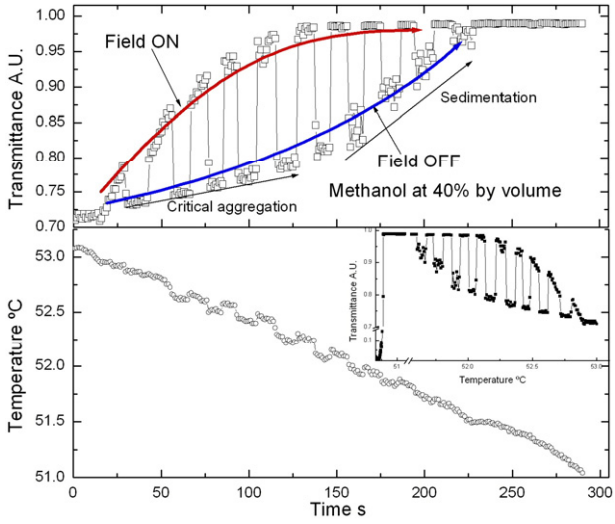

Figure 1. Temporal evolution of the optical transmittance (upper panel) and temperature (lower panel) as a periodic magnetic field is applied starting above the demixing temperature until demixing is completed. The inset shows the transmittance as a function of the actual temperature of the sample.

aggregate irreversibly and precipitate when separation of the mixture takes place, inducing aging of our samples. These precipitates usually rest at the interface after the demixing transition has occurred, but the density of this phase can be large enough to overcome the density of the methanol-rich phase, and then precipitate down to the bottom of the test tube. In order to understand this aging mechanism and aggregation dynamics, and the true capacity of shifting the coexistence curve by means of an external magnetic field, we designed a series of dynamic experiments, with fresh samples for each run.

As is well known, the critical temperature of a binary mixture can be noticeably shifted even with minute amounts or traces of water or doping compounds, so a great deal of care in sample preparation is needed to attain reproducibility in measuring coexistence curves.

Transmittance measurements were done using a square wave magnetic field with a field amplitude of 80 Oe and a period of 20 s, which was applied to a fresh sample during the cooling ramp that began at a temperature of a few degrees above the separation temperature and stopped once the separation itself took place. The rich phenomenology observed in this series of experiments is of great interest and represents the main issue that we want to address in this paper in order to open up the discussion not only on critical Casimir forces, but on the coupling of two different kinds of transitions: a coupling that can enhance optical and thermal properties, or provide control knobs for a set of parameters of one transition over the parameters of the other.

3. Experimental findings and discussion

In figure 1 we present the results of a typical experiment in which both the transmitted light intensity (upper panel) and the

temperature readout (lower panel) measured during the cooling ramp in a mixture sample of 40% of methanol is shown.

In the upper panel of figure 1, the main features observed, which we identify with a reversible chain forming process and with critical aggregation phenomena, are clearly seen as enveloping curves of the optical signal. In this graphic, the transmittance and the cooling ramp are displayed as a function of time.

The experiment initiates at a temperature well above the coexistence curve. As time elapses, the temperature decreases; approaching the separation temperature T_s which is located approximately at 50.65 °C (shown in the inset) as the magnetic field is switched on and off alternating in order to measure the magnetically induced changes in transmittance. Initially, above and far from T_s, the transmitted light intensity shows little change in response to the applied field. However, as the temperature gets closer to T_s, the turbidity of the mixture begins to show increasing changes with the applied field. In particular, the transmittance (or the transmitted divided by the incident light intensity values) increases when the magnetic field is switched on. This can be observed in the upper panel of figure 1, where the difference in transmittance between the field-off and field-on states, indicated as red and blue lines, respectively, first increases until approximately 150 s and then decreases as the temperature diminishes towards T_s. In the inset of figure 1, the transmittance as a function of temperature is shown for even larger times (about 400 s) for which the phase separation undergoes at 50.6 °C and transmittance goes close to zero.

Considering in more detail the trends in the temporal evolution of the field-off and-on states, we can see that the field-off state evolves by firstly showing a slow increase, almost linear, up to approximately 150 s, followed by a more steep variation. For the field-on state, the increase shows a larger slope, which is almost linear and then, at approximately 100 s, slows down and finally shows a saturation effect in which, for this state, the light intensity remains constant.

These trends have been interpreted in terms of a reduction in the number of scattering centers due to aggregation of the incipient heterogeneous nuclei of the two new phase embryos, but with increasing changes in transmission intensity that are observed in response to the external field due to a chain-like flock formation of the magnetic particles. Thus, the envelope of the light intensity curve is constituted by two main aggregation curves that we will call from here on: critical (which will lead to irreversible aggregates if temperature gets very close to demixing) aggregation for the field-off curve, and the magnetic reversible aggregation curve for the field-on curve. These two enveloping curves carry complementary information about these coupled transitions, being; (a) the critical demixing transition and (b) the order–disorder transitions of chain-forming particles in response to the applied external field.

The above stated time of 150 s marks the onset for which the field-off curve shifts from a smooth slope to a more pronounced one and is related to the precipitation of particles that start to settle down due to their large size, as discussed below, which results in the decrease of the number of magnetic particles in the optical exploration region. The transmittance further continues to increase until saturation of the detected signal occurs.

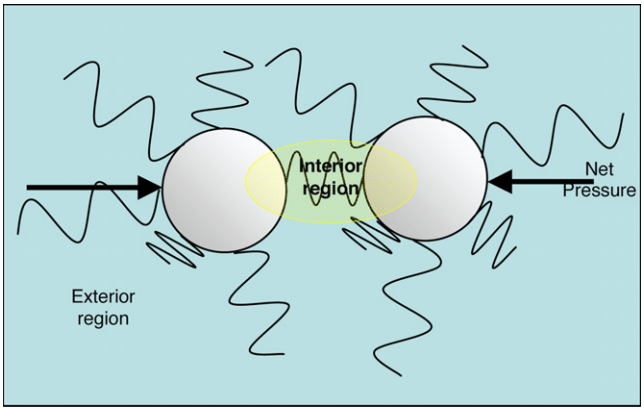

Figure 2. Physical picture explaining the origin of critical Casimir attraction among colloids.

The critical demixing transition is characterized by diverging fluctuations (correlation length) in composition and thus, increasingly, heterogeneities in density and refractive index develop as the system approaches the coexistence curve. Heterogeneous nucleation of the new cyclohexane phase proceeds due to the presence of magnetic nanoparticles which are preferentially wetted by this phase, phenomenon called the wetting transition which always precedes the demixing of the mixture [13]. While temperature is further lowered these nuclei form stable embryos as they reach a critical radius at which effects of enhanced vapor pressure (due to small curvature radii) and surface tension allows stability and growth. At this point, phase separation starts, accompanied by a strong scattering of light—critical opalescence—since the embryos have evolved to true droplets of the new phases having wavelength-like sizes. This cloudy point occurs in figure 1 for very large times and is evident in the inset for a temperature of approximately 50.65 °C.

Fluctuations among magnetic particles, or embryos, produce an effective attraction between them, since their presence represents boundary conditions that limit the normal modes of the liquid phase within the gap between particles. Given that the vast majority of these modes are inhibited in this gap, the 'radiation pressure' exerted by surrounding fluctuations (the whole number of modes are present in the external region, see figure 2) exceeds the one pushing apart both particles, resulting in a net attractive force proportional to the magnitude of the fluctuations. Since the correlation length of fluctuations diverges as the critical temperature approaches, so does the attractive force between suspended particles—hence, the critical Casimir forces. In this sense, any kind of colloidal stabilization mechanism can be overtaken by Casimir-like attractions and coagulation will take place. Relevant Casimir attractions (larger than $k_B T$) were predicted just for reduced temperatures of a small fraction of a degree celsius, contrary to our observations in which critical aggregation starts a few degrees above the demixing transition. This long range attraction is still subject to debate and has

been attributed to effects such as a bridging transition [14] (in our case, bridging is unlikely since this should only apply for $T < T_c$ in the bimodal region), up to a dramatic Debye screening length reduction due to the adsorption layer of the preferred phase which can destabilize the repulsive barrier and in turn the suspension itself, leading to critical coagulation [15, 16]. However, very recently Bonn *et al*, reported direct confocal observations in index-matched critical suspensions of Teflon spheres in order to measure the Casimir and electrostatic contributions to critical aggregation and found critical Casimir aggregation for an extremely large window of 15 °C in agreement with our observations [17].

In colloidal science, a large variety of schemes have been developed in order to manipulate at will colloid–colloid interactions (salt addition, refractive index matching, polymer coating of particles in brush-like fashion, etc), schemes that are well described and modeled by the Derjaguin, Landau, Verwey and Overbeek or DLVO theory of colloidal stability. However, suspensions of colloids in critical mixtures are suitable to probe and tune the interaction potential by simply adjusting the temperature and this has led us to show recently their versatility in controlling crystallization [16, 17] or preferential adsorption on patterned surfaces [18].

The critical coagulation process actually can be observed by changes in turbidity since the light scattering centers become more efficient as their size grows closer to the wavelength of the probing radiation. Turbidity measurements are well suited for exploring the aggregation dynamics since dynamic light scattering can be used just for temperatures well above the transition since this technique requires large averaging or integrating times in order to get reasonably well-defined sizes for the nuclei. As stated above, the critical aggregation curve or lower envelope in figure 1 has a small slope for temperatures far from T_s that, afterwards, starts to increase at about 150 s (51.9 °C). However, these small changes in transmitted intensity induce increasing changes in the reversible aggregation envelope (upper part). These larger changes in turbidity observed when the magnetic field is turned on reveal the chain formation oriented in the direction of the light propagation vector in a Faraday configuration experiment. Besides, these chains become stiffer and easier to form as the constituent particles become gradually larger due to critical aggregation (dipole–dipole interaction scales as the square of the magnetization), and in turn their effective scattering section diminishes as temperature approaches T_s. Since the number of scattering centers is reduced by critical aggregation, combined with the orientational self-shading effect caused by dipole–dipole aggregation, self-shading in this Faraday configuration becomes more efficient, causing increased transmittance in response to the applied field.

From figure 1, it is clear that both aggregation mechanisms are mutually independent since they recover their own tendency in a continuous and soft fashion, once the external field condition recovers its original value. These two aggregation mechanisms can be interpreted as a critical Casimir driven (irreversible for temperatures close enough to T_s) and a magnetically driven (always reversible) phenomenon since the upper and lower envelopes represent the chain forming process and the formation of large spherical aggregates that eventually precipitate down, as we shall discuss later in this paper, respectively. We should be clear that the critical Casimir aggregation is considered irreversible just if the demixing temperature is surpassed, as it occurred in this series of experiments, but reversibility far from T_s is possible, as described by Beysens [13] and very recently by Bonn [17], but was not tested in this report.

This means that, in spite of sudden changes induced by applying the external magnetic field, the growth tendency of the chains or the individual links is always recovered when the field is turned off. However, it must be remarked that, for the upper part of the envelope, there is a saw-tooth behavior that can be easily understood if we consider the nonlinear chain formation dynamics caused by a larger attraction of free particles towards larger chains that have a larger dipolar moment and the depletion of magnetic particles in the surrounding region of a chain due to the chain formation itself [19]. Then, each time the field is turned off the chains are destroyed by thermal motion and they have to reform; during a new event of application of the external field, they first have to reach the values of chain length (and optical dispersion power) they had in the last part of the previous cycle prior to continuing their growth, giving the characteristic saw-tooth growing behavior seen in the optical signal.

A simple interpretation of the transmitted light intensity is a complex task. A vast wealth of phenomena are involved in the final scattered light signal going from the size of the dispersed particles, the temperature—which not only promotes strong fluctuations but in turn promotes changes in the size of the suspended particles by critical aggregation, the magnetic field and its orientation, the stiffness of the formed chains and the rate at which the temperature is changed.

A glance at the complexity that represents the measured optical signal can be seen in figure 3, where three curves of transmittance versus temperature are presented for different cyclohexane–methanol compositions.

In the upper panel of figure 3(a), the transmitted intensity is shown for a composition containing 32% of methanol (68% cyclohexane) and here the critical aggregation envelope is the upper curve, while the magnetic reversible aggregation corresponds to the lower enveloping curve. In contrast, the lower panel or figure 3(c)—corresponding to 44% of methanol—presents an irreversible aggregation curve located as the lower envelope and a magnetic reversible envelope is coming from above. Indicating that chain formation in response to the external magnetic field can induce changes in transmittance in both directions, increasing or diminishing it, depending on the composition of the sample or even on their proximity to the coexistence curve and the cooling history of the sample. For the middle panel of figure 3(b) in which the optical transmitted signal for 40% methanol as a function of temperature is shown, a crossover between these two behaviors is seen; the magnetic aggregation envelope starts for high temperatures diminishing the transmittance of the mixture and changes to increasing it for temperatures below 50.85 °C where the crossover sets in and almost any changes in optical transmission are produced by applying the external magnetic field.

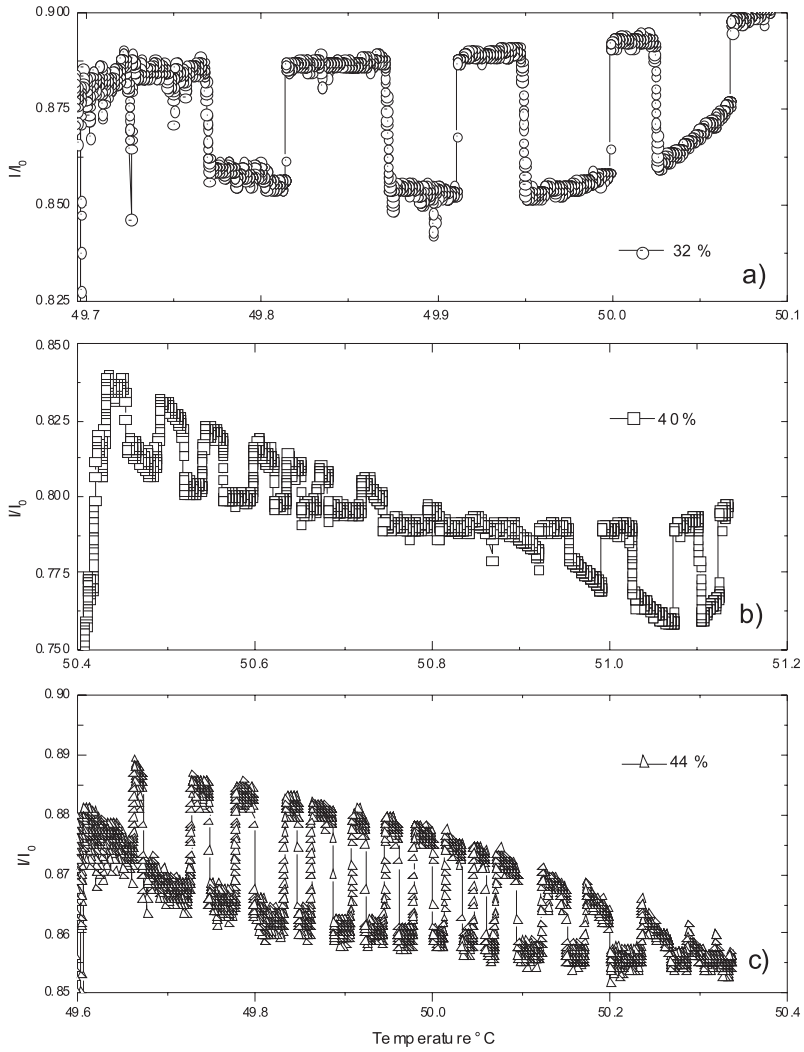

Figure 3. Transmittance as a function of temperature for three different compositions; the upper panel (a) shows a decreasing transmittance, while in the lower panel (c) the transmittance is increased in response to the field for volume fractions of 32% and 44% of methanol, respectively. In the middle panel (b) both increasing and decreasing transmittance can be appreciated for an intermediate composition of 40% of methanol/volume.

Several hypotheses could be proposed to explain these different regimes in which a better (hindered) light transmission is induced by means of turning on (off) the magnetic field. For example, far from T_s, one could imagine the suspended nanoparticles forming very small chains that are easily bent by thermal agitation and presenting an effective scattering cross section that increases with the chain length (due to strong Landau–Peierls fluctuations that confers on them a large bending tendency when magnetic particles are still small). However, the size of their constituent links grows as the cooling proceeds, depleting the suspended particles and simultaneously increasing the rigidity of the chains, leading to a state in which chains oriented in the direction of light propagation reduce the effective scattering cross section of the suspended phase. In other words, as particles form straighter chains and these chains sequester the surrounding magnetic nanoparticles, the number of effective scattering centers is reduced and the transmitted intensity consequently grows. Here we should point out that temperature [19] can both; decrease the magnetic-field-induced optical transmittance in colloidal suspensions when the stochastic force of thermal fluctuations dominates the dipolar forces, or increase the optical transmittance by annealing away defects when dipolar and thermal forces are comparable. However, in our case the stiffness of the forming chains is increased as temperature diminishes not only by the consequent reduction in the thermal fluctuations but also due to the growing size of the chain constituent links by critical aggregation, but annealing cannot be evoked in the present work. Thus, for certain temperatures (considering as well the thermal history of the sample such as the cooling ramp slope and time spent close to the demixing transition) the chains, viewed as columns in the direction of light beam propagation, will reach a point for which the magnetic induced optical transmission will change from hampering it to improving it. At this point, an adimensional reduced temperature $J = k_B T/B^2 a^3$, B being the magnetic field, should be close to one due to a large particle size a and the average scattering cross section of bent chains should

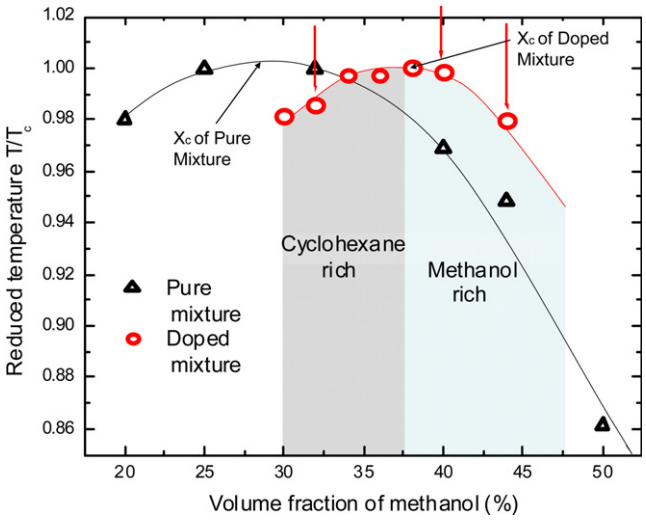

Figure 4. Phase diagram in composition and reduced temperature for the doped and undoped binary mixture. The arrows indicate the 'pathways' or cooling ramps followed in the experiments shown in figures 1 and 3.

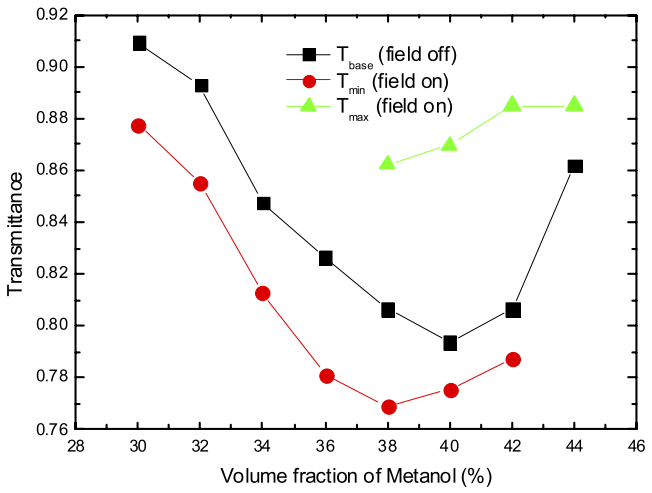

Figure 5. Maximum (green triangles) and minimum (red circles) transmittance values observed in response to the magnetic field application for different compositions of the binary mixture. The black squares show the transmittance value of the mixture with the field turned off for the temperature at which maximal changes were observed for each composition.

equal the effective scattering area of the random distribution of isolated particles.

A survey of the phase diagram is presented in figure 4, in which the pure mixture coexistence curve is depicted together with the coexistence curve of our doped system. Both are rescaled and presented in terms of their corresponding reduced temperature for a better comparison. Here a shift in the critical composition X_c towards more rich methanol compositions (right) can be observed, being approximately 28 and 38% by volume of the critical compositions for the undoped and doped systems, respectively. The continuous lines are just guides to the eyes.

Composition is important as well due to the wetting preference for CH of the magnetic nanoparticles as has been well established since Beysens' work [3]. It is worth noting that changes in transmittance in response to the applied field were observed just for the methanol-rich side (in volume) of the phase diagram of the pure mixture. For particles in samples with plenty of cyclohexane (CH-rich side of the doped phase diagram), the mixture tends to decrease its transmittance as chains form in response to the field close to the demixing transition. However, in samples in the methanol-rich side of the doped phase diagram the tendency is in the opposite direction increasing the transmittance as the chains form, and there is an intermediate region close to the critical composition for which both behaviors can be observed as shown in figure 3.

This behavior is better explained by seeing figure 5 in which the initial transmittance baseline is plotted as black squares as a function of the volume fraction of methanol of the sample. By red circles, we have plotted the maximum change (decreasing of the transmitted intensity), or the maximal vertical distance between the two enveloping components added (in this case subtracted) to the reference baseline, a change induced by the magnetic field application during the experiment. By green triangles, the same maximal distance between the critical and magnetic chain aggregation envelopes added to the reference baseline of the initial transmission intensity is plotted. In this case, the changes observed are such that the transmitted intensity increases when the magnetic field is applied. As can be observed, there is a region (0.38, 0.42) in which both increasing or decreasing of the signal intensity occurs in response to the magnetic field. We should point out that, in this overlapping region, the transmittance is always reduced in response to the magnetic field for temperatures far from the separation temperature and is increased for temperatures closer to the separation temperature as seen in figure 3(b).

The behavior of the optical signal in both directions—increasing or decreasing the transmittance in response to the field—is clearly associated with the composition of the mixture. As can be seen from figures 4 and 5, the maximal change induced in the optical signal by the field resembles the inverted phase diagram of the doped mixture. To make this more evident, in figure 6 we have plotted by crossed triangles the doped phase diagram of our mixture together with the reciprocal of the maximal intensity deviations normalized (or divided) by the maximum value of them, as circles and triangles corresponding to those in figure 5. A good correspondence between the coexistence curve and this 'reduced maximal intensity deviation' is seen on the cyclohexane-rich side, indicating that the scattering mechanism induced by the field in this side of the phase diagram is the same as the scattering mechanism that is going on during the process of phase separation, being isotropic in nature. Availability of cyclohexane (larger partial pressure of this phase) allows the tiny magnetic particles to easily nucleate the cyclohexane-rich new phase and the magnetically induced aggregation will make them coalesce, bend and entangle as a mop, due to thermal and surface tension effects. This process is seen as an isotropic growing of nuclei by the light probe and thus the transmittance is lowered. Due to these magnetically

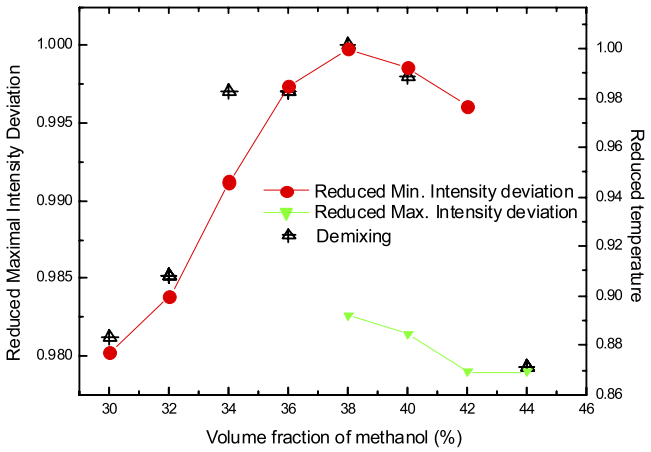

Figure 6. Reduced temperature versus composition phase diagram plotted as crossed triangles (right vertical axis) and reduced maximal intensity deviation plotted as circles and inverted triangles (left axis) showing a closely related mechanism in the optical changes that allow us to track the demixing transition and the magnetically induced changes in the optical signal in the CH-rich side of the phase diagram.

induced larger scattering centers, the sample behaves as if it was closer to the demixing point and the optical signal follows the coexistence curve.

On the other side of the phase diagram, magnetic nanoparticles can hardly nucleate cyclohexane nor methanol embryos due to their preference for cyclohexane and the larger partial pressure of methanol, and thus, easily aggregate in stringy flocks in response to the field, since the only competing force comes from thermal fluctuations. These flocks are elongated in the direction of propagation of the light probe and effectively diminish the total scattering cross section in the exploration region. Thus, the anisotropic nature of this magnetically induced aggregation leads to the observed increasing in transmittance, which has no reason to be directly mapped into the coexistence curve of the phase diagram but in a marginal way.

During the whole separation process of the binary mixture, the otherwise stable suspension of magnetic nanoparticles undergoes critical Casimir aggregation and subsequently Casimir coagulation, processes in which magnetic nuclei continually grow until they become unstable and precipitate. The precipitated particles appear as a brownish scum at the cyclohexane-rich/methanol-rich interphase. By means of a Pasteur pipette, a sample of this scum has been removed and further analyzed by scanning electron microscopy (SEM); pictures are shown in figure 7. Here, very interesting structures can be appreciated, in which the aggregation process history remains recorded. A large distribution of spheres, ranging from half a micron up to 30 μm, is formed due to heterogeneous nucleation as can be seen in figure 7(a). In figure 7(b) a detail of a large broken sphere is shown, having a nutshell structure with many small spheres in its interior. This is the signature of double emulsion formation during the demixing transition in which magnetic particles and their stabilizing agents act as surfactants that can develop a certain rigidity due to diverging Casimir forces which bring the building blocks together and finally allows the van der Walls forces to tightly cement these bricks jointly. Double emulsions in critical mixtures undergoing separation, can thus be viewed as a good prospect to encapsulate active components in hard magnetic microspheres, for targeted drug delivery, but further investigation in this direction is needed. Finally it should be noted that, despite large changes in the optical signal for the off or on field states for temperatures above the coexistence curve, the phase diagrams obtained with fresh samples with the field kept on or off during the whole experiment do not show any significant shift of the coexistence curve. In other words, the transition takes place at the same temperature no matter if the field is turned on or off because critical Casimir flocculation overcomes magnetic processes close to demixing.

So far, the magneto-optic effects prevailing in magnetically doped binary mixtures close to separation and the signature of critical aggregation as well as Casimir forces in the transmitted light intensity signal have been discussed. However the separation process is energetically very demanding (large enthalpies of demixing) which is not the case for the ordering transition of chain forming systems such as a ferrofluid. Until now, just a few degrees celsius under ambient temperature can be achieved using magnetocaloric ceramics and the Debye adiabatic demagnetization has been used solely in low temperature systems to reach millikelvin

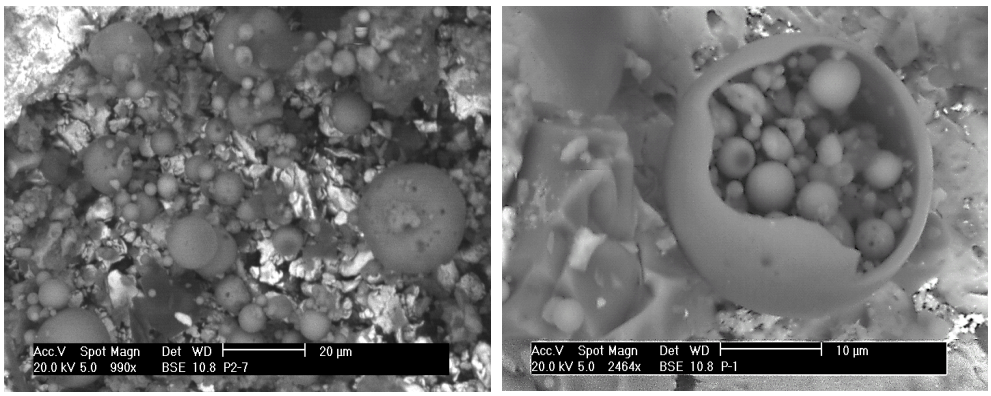

Figure 7. Scanning electron micrographs showing; (a) the spherical morphology of the aggregates and the broad distribution of sizes, and (b) the nutshell-like structure of a large aggregate and the smaller aggregates crowding its interior.

temperatures. In this sense, the possibility of coupling the magnetic ordering to the mixing transition in order to enhance or inhibit separation by means of imposing an external magnetic field seems to be promising in developing nonsolid state magnetocaloric systems with higher energies involved in the magnetic ordering or chain forming processes. This phase transition coupling (magnetic ordering and demixing) can actually enhance the thermocaloric effect. This can be clearly seen in the lower panel of figure 1 in which the thermometric signal coming from the thermocouple, situated in the bath close to the sample, is plotted as a function of time and the optical signal is shown in the upper panel of the same figure 1 as it was acquired (also as a function of time). Strikingly, synchronous jumps in the optical and thermal signals are detected, being of the order of a tenth of a degree celsius for the temperature shift as the magnetic field is turned on (off). Intermixing of electrical signals or induction phenomena were discarded, using pure water samples where no effect was observed, and looking at larger times where the separation takes place, separation which induces a more pronounced cooling rate (not shown). We should point out that, even if this change in temperature seems to be small, a large amount of heat is involved since the thermal bath contains at least twenty times the volume of the sample in water. Further calorimetric measurements are needed to determine the heat involved during each single event of turning on the magnetic field. However, a rough estimate indicates that we have 1 J g^{-1}, as 100 g of water increases or decreases its temperature 0.1 °C by switching on or off the 80 G magnetic field—considering a heat capacity of 4.18 J g^{-1} K^{-1}—it represents a 4.1 J liberated by an amount of about 4 g of mixture, which has a heat of mixing of about a couple of hundreds of calories per mol—[20]. In contrast, the giant magnetocaloric effect [21] implies a heat of about 10 J kg^{-1} K^{-1} for 0–5 T magnetic fields.

A simple physical picture suggests that the chain forming process induces changes in the geometry and surface of the embryos that have formed as the system approaches the separation temperature. Here a set of embryos surrounding the magnetic particles are first uniformly distributed in the mixture, but in response to the imposed magnetic field, these embryos will migrate towards a chain (partially depleting the bulk and forming channels) and coalesce with close neighbors to form a nonspherical cylindrical embryo. These cylindrical embryos have a smaller and more stable surface and the energy excess associated with a lager surface is liberated as heat. Conversely, when the field is turned off, thermal agitation destroys the already formed chain-shaped embryos, generating new surface to individually cover the newly disaggregated embryos. Formation of this new surface requires a certain amount of energy taken from the medium which cools down the sample. As clearly seen from figure 1, not only the jumps in temperature are synchronized with the magnetic field application, but also the growth (decrease) in the optical signal (transmittance). This is a clear signature of a novel magnetocaloric effect in which magnetic chain formation drives changes in the total surface of the embryos, and as a consequence with the scattering effective area of these nuclei or scattering centers.

4. Conclusions

In summary, we have presented turbidity measurements of a partially miscible mixture of cyclohexane and methanol, close to demixing, doped with superparamagnetic nanoparticles of a commercial ferrofluid in response to an external, uniform and low intensity magnetic field. Magneto-optical and magnetocaloric effects were observed and interpreted in terms of the coupling between the demixing and ordering (chain forming) transitions, which has not been reported previously. For more CH-rich compositions, the magneto-optical effect is such that the measured transmittance is increased in response to the application of a uniform magnetic field and, on the other side, for more methanol-rich compositions, the magneto-optic effect evolves in the opposite sense, decreasing the transmittance of the sample as the external field is applied. Interestingly, we have observed for intermediate compositions that the optical effect appears in both directions—increasing transmittance of the sample in response to the application of the field for temperatures closer to T_s and decreasing the transmitted intensity for temperatures far above the demixing curve. Noticeably the magneto-optic effect is canceled for certain temperatures due to competing effects of increasing turbidity as the system approaches T_s and reduction (increment) of the dispersion power of the scattering centers as they grow and reorganize to form stiffer dipolar chains. Coupled to the magneto-optical effect, evidence of a magnetocaloric effect was found in the temperature signal of the thermal bath. It is suggested that the magnetic field application drives changes in the total interface between the forming embryos of the CH-rich phase—which covers the magnetic particles when they cluster together for chain forming—and bridging spherical surfaces to form instead cylindrical-like embryos and freeing energy in the process.

The rich phenomenology found in this system opens up a myriad of questions yet to be solved on the origin and dynamics of aggregation of magnetic colloids in binary mixtures and a possibility to chemically engineer magnetic colloidal suspensions in critical mixtures to profit from this newly and enhanced magnetocaloric effect.

Acknowledgments

This project was partially founded by CONACYT grant no. 82975 and UASLP C08-FAI-04-17.21. LH-D thanks CONACYT for support through a scholarship. Thanks to J Carlos Ornelas-Lizcano for help setting up the data acquisition system, Roger Vega-Acosta for the zeta potential measurements and Nubia Arteaga-Larios for the pictures at SEM.

References

[1] Casimir H B G and Polder D 1948 *Phys. Rev.* **73** 360
[2] Schlesener F, Hanke A and Dietrich S 2003 *J. Stat. Phys.* **110** 981
[3] Beysens D and Esteve D 1985 *Phys. Rev. Lett.* **54** 2123
[4] Hertlein C, Helden L, Gambassi A, Dietrich S and Bechinger C 2008 *Nature* **451** 172

[5] Tsori Y, Tournilhac F and Leibler L 2004 *Nature* **430** 544
[6] Odenbach S (ed) 2003 *Ferrofluids: Magnetically Controllable Fluids and Their Applications* (*Lecture Notes in Physics* vol 594) (New York: Springer) p 253
[7] Rosensweig R E 1985 *Ferrohydrodynamics* (Cambridge: Cambridge University Press) p 344
[8] Giauque W F and MacDougall D P 1933 *Phys. Rev.* **43** 768
[9] Mella S, Rubio M A and Fuller G G 2001 *Phys. Rev. Lett.* **87** 115501
[10] Zemansky M W 1981 *Temperatures Very Low and Very High* (New York: Dover) p 50
[11] Pecharsky V K and Gschneidner K A Jr 1997 *Phys. Rev. Lett.* **78** 4494
[12] Pang C P, Hsieh C T and Lue J T 2003 *J. Phys. D: Appl. Phys.* **36** 1764–8
[13] Beysens D and Narayanan T 1999 *J. Stat. Phys.* **95** 997
[14] Archer J, Evans R, Roth R and Oettel M 2005 *J. Chem. Phys.* **122** 084513
[15] Law M, Petit J-M and Beysens D 1998 *Phys. Rev.* E **57** 5782
[16] Guo H, Narayanan T, Sztuchi M, Schall P and Wegdam G H 2008 *Phys. Rev. Lett.* **100** 188303
[17] Bonn D, Otwinowski J, Sacanna S, Guo H, Wegdam G and Schall P 2009 *Phys. Rev. Lett.* **103** 156101
[18] Soyka F, Zvyagolskaya O, Hertlein C, Helden L and Bechinger C 2008 *Phys. Rev. Lett.* **101** 208301
[19] Martin J E, Hill K M and Tigges C P 1999 *Phys. Rev.* E **59** 5676
[20] Wood S E 1946 *J. Am. Chem. Soc.* **68** 1963
[21] Pecharsky V K and Gschneidner K A Jr 1997 *Phys. Rev. Lett.* **78** 4494